ISSN 0036-0236, Russian Journal of Inorganic Chemistry, 2019, Vol. 64, No. 8, pp. 1063–1071. © Pleiades Publishing, Ltd., 2019.

INORGANIC MATERIALS AND NANOMATERIALS

Cadmium Chloride and Cadmium Iodide Thiosemicarbazone Complexes as Single Source Precursors for CdS Nanoparticles

Siphamandla C. Masikane[a], Sixberth Mlowe[a, *], Amol S. Pawar[b], Shivram S. Garje[b], and Neerish Revaprasadu[a]

[a] *Department of Chemistry, University of Zululand, Private Bag X1001, Kwa-Dlangezwa, 3886 South Africa*

[b] *Department of Chemistry, University of Mumbai, Vidyanagari, Santacruz (E), Mumbai, 400098 India*

**e-mail: sixb2809@gmail.com*

Received February 1, 2018; revised October 25, 2018; accepted April 15, 2019

Abstract—Cadmium sulfide (CdS) nanoparticles have been synthesized from CdX_2 ($X = Cl^-, I^-$) complexes of 4-chlorobenzaldehyde and benzophenone thiosemicarbazone. The complexes have been studied by thermogravimetric analysis (TGA), elemental analysis, FT-IR, and NMR spectroscopy. The solvothermal decomposition of the complexes has afforded oleylamine-capped CdS nanoparticles with a wurtzite hexagonal phase. The transmission electron microscopy (TEM) studies show different morphologies which are influenced by reaction temperature and the nature of the ligands on the precursor complexes. Particles in the form of irregular cubes, elongated cubes and nanodendrites have been observed. The UV-Vis spectroscopy measurements show temperature and nature of complex-dependant optical properties. Blue-shifted band gap energies have been observed at lower reaction temperatures.

Keywords: single source precursors, thiosemicarbazone, nanodendrites, solvothermal synthesis, cadmium sulphide

DOI: 10.1134/S0036023619080072

Group II–VI semiconductor nanomaterials have interesting properties which make the exploitable in various industrial applications. The tunability of these properties through the manipulation of synthetic procedures has ensured that interest in this area is maintained. Controlling the particle size and shape is a simple means to manipulate the properties of the materials. Cadmium sulfide (CdS) with its tunable direct band gap (2.42 eV) is a widely studied material [1]. There has been an exponential increase in the fabrication of CdS nanoparticles (NPs) exhibiting different morphologies such as nanospheres, nanorods, nanoflowers and nanoplates [2–5]. Depending on the particle size, shape and morphology, CdS NPs find applications in solar cells, gas sensors, light emitting diodes, flat panel displays, and catalysis [6–9]. Despite their toxic nature, CdS NPs have also been identified as promising materials for the environmental remediation such as the catalytic degradation of organic dyes from industrial waste [10]. Furthermore, the scope of the study extends to evaluating the interaction of these NPs in biological systems; from cytotoxic effects [11] to tumour detection [12] and targeted drug delivery [13].

Various fabrication methods have been reported to afford high quality CdS NPs. The most common methods such as hot-injection [14], precipitation [15] and microwave irradiation [16] are usually solvent-based, thus, allowing the stabilisation of the NPs during and after completion of particle growth assisted by coordinating solvents. There is a wide range of coordinating solvents which contain functional groups that facilitate the solubility of the NPs in a medium of choice, e.g. L-cysteine [17] for water soluble NPs intended for biological applications, while long chain amines and phosphines are commonly used for organic solvent soluble NPs [14]. Furthermore, it has been established that the coordinating solvent plays a crucial role in controlling the particle size, shape and morphology [18, 19]. The synthetic methods also provide the ability to tune the properties of the NPs through the variation of reaction parameters such as type and concentration of precursors, reaction temperature and reaction time.

As a result of environmental concerns and awareness, there has been an increase in devising and practicing alternative green protocols for nanomaterials synthesis [20]. The different approaches reported; focus on using either solvents or precursors which are eco-friendly. Our group have reported the green synthesis of cadmium and lead chalcogenide NPs using olive oil, castor oil, ricinoleic acid, anacardic acid extracts as coordinating solvents [10, 21–23]. The use of metal complexes as single-source precursors has

advantages over multiple source precursors [24]. The pre-existing bonds in the complexes facilitate clean decomposition. In the case of CdS NPs, the use of dithiocarbamate [10, 21, 25–27], xanthate [14, 28], thiobiuret [29], thiourea [30] and thiophosphinate [31] complexes are well reported. A study conducted by O'Brien and co-workers [32] revealed that the alkyl chain lengths of lead(II) alkyl xanthate complexes had an influence on the size and shapes of the PbS nanocrystal formed.

We have recently reported the synthesis of CdS nanoparticles using floroacetophenone and cinnamaldehyde thiosemicarbazone cadmium complexes [33]. In the study, the effect of halogen composition in the single source precursor strongly influenced the morphological and optical properties of the as-synthesized CdS nanoparticles. In this paper, we report the use of benzophenone and 4-chlorobenzaldehyde thiosemicarbazone ligands which are structurally different from the earlier work, for synthesizing complexes incorporating $CdCl_2$ and CdI_2. We wanted to investigate the influence of the nature of the ligands and reaction temperature, in addition to iodide/chloride inclusion in the single source precursor as a primary objective, on the morphological and optical properties of the CdS nanoparticles.

EXPERIMENTAL

Materials and Measurements

Tri-*n*-octylphosphine and oleylamine were purchased from Sigma-Aldrich. Acetone, methanol, cyclohexane and hexane were obtained from Shalom Laboratories. Cadmium chloride and cadmium iodide were purchased from S D Fine-Chem. Limited. All chemicals were used as received. Elemental analysis for carbon, hydrogen, nitrogen and sulfur were carried out with a Thermo Finnigan Italy Model FLASH EA 1112 Series elemental analyser. Quantitative determination of cadmium and chloride contents were performed by complexometric and Volhard titration methods, respectively. IR spectra were recorded on a Perkin-Elmer Spectrum One FTIR Spectrometer in the range 4000–400 cm^{-1}. TGA measurements were performed using a PerkinElmer Pyris Diamond TG/DTA model from 30 to 600°C at a heating rate of 10 K min^{-1} under nitrogen atmosphere. ^1H and ^{13}C (^1H) NMR spectra were recorded with a Bruker 300 MHz spectrometer at room temperature using DMSO-d_6 as a solvent and TMS as an internal reference. UV-Vis absorption spectra were recorded on a Varian Cary 50 UV/Vis spectrophotometer using a quartz cuvette (1 cm path length) and hexane as a dispersing solvent. JEOL 1400 (120 kV) and JEOL 2010 (200 kV) were used to record TEM and HRTEM images, respectively. Powder XRD patterns were recorded at room temperature using a Bruker AXS D8 Advance diffractometer equipped with nickel-filtered Cu-Kα radiation (λ = 1.5418 Å) at 40 kV and 40 mA.

Synthesis of Complexes

4-Chlorobenzaldehyde thiosemicarbazone and benzophenone thiosemicarbazone ligands were prepared by methods reported elsewhere [34].

Preparation of bis(4-chlorobenzaldehyde thiosemicarbazone)cadmium(II) chloride (1). 4-Chlorobenzaldehyde thiosemicarbazone (0.946 g, 4.42 mmol) was dissolved in anhydrous methanol (20 mL). To the resulting solution was added $CdCl_2$ (0.406 g, 2.21 mmol) dissolved in anhydrous methanol (20 mL) with constant stirring, which was continued for 36 h at room temperature. The solvent was evaporated in vacuo to give a white precipitate, which was washed with cyclohexane (3 × 10 mL), followed by of n-hexane (2 × 10 mL) to remove any impurities, and dried in vacuo to afford analytically pure product **1**, yield 1.165 g (86.16%), mp 221°C.

For $CdCl_4C_{16}H_{16}N_6S_2$ calculated, %: Cd, 18.40; C, 31.46; H, 2.64; N, 13.76; S, 10.50; Cl, 23.21.

Found, %: Cd, 18.73; C, 31.76; H, 2.48; N, 13.49; S, 10.22; Cl, 23.01.

IR, cm^{-1}: 3451, 3296 (ν_{NH_2} asymm. and symm.), 3188 (ν_{N-H}), 1589 (ν_{C-N}), 957 cm^{-1} (ν_{C-S}).

^1H NMR (δ, ppm): 7.42–8.31 (s, NH_2, mC_6H_5–CH=N), 11.57 (s, NH), ^{13}C NMR (δ, ppm): 177.47 (C=S), 141.41 (CH=N), 134.32, 133.01, 128.95, 128.66 (aromatic carbons).

Preparation of bis(benzophenone thiosemicarbazone)cadmium(II) chloride (2). The reaction protocol for **1** was followed. Benzophenone thiosemicarbazone (1.317 g, 5.16 mmol) and $CdCl_2$ (0.473 g, 2.58 mmol) gave a white precipitate of **2**, yield 1.614 g (90.16%), mp 194°C.

For $CdCl_2C_{28}H_{26}N_6S_2$ calculated, %: Cd, 16.19; C, 48.45; H, 3.77; N, 12.10; S, 9.24; Cl, 10.21.

Found, %: Cd, 16.53; C, 48.77; H, 3.52; N, 12.29; S, 9.05; Cl, 10.42.

IR, cm^{-1}: 3399, 3287 (ν_{NH_2} asymm. and symm.), 3167 (ν_{N-H}), 1602 (ν_{C-N}), 837 (ν_{C-S}).

^1H NMR (δ, ppm): 7.30–8.53 (s, NH_2, mC_6H_5–C=N), 8.63 (s, NH); ^{13}C NMR (δ, ppm): 177.56 (C=S), 149.54 (C=N), 136.25, 131.17, 129.97, 129.77, 128.32, 128.25, 127.57 (aromatic carbons).

Preparation of bis(4-chlorobenzaldehyde thiosemicarbazone)cadmium(II) iodide (3). The reaction protocol for **1** was followed. 4-chlorobenzaldehyde thiosemicarbazone (0.869 g, 4.06 mmol) and CdI_2 (0.745 g, 2.03 mmol) gave a white precipitate of **3**, yield 1.483 g (91.88%), mp 218°C.

For $CdI_2Cl_2C_{16}H_{16}N_6S_2$ calculated, %: Cd, 14.16; C, 24.21; H, 2.03; N, 10.58; S, 8.08; Cl, 8.93.

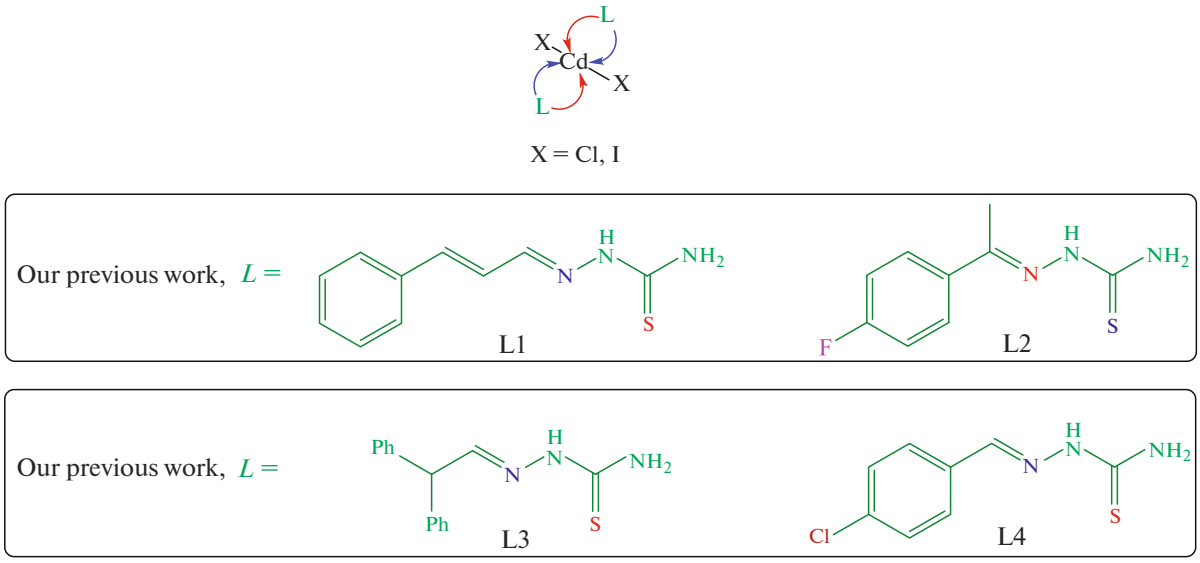

Fig. 1. Structural representation of the single source precursors used in the previous and current work, to prepare CdS NPs.

Found, %: Cd, 14.32; C, 24.56; H, 2.28; N, 10.32; S, 7.85; Cl, 8.64.

IR, cm^{-1}: 3412, 3262 (ν_{NH_2} asymm. and symm.), 3156 (ν_{N-H}), 1588 (ν_{C-N}), 955 (ν_{C-S}).

^1H NMR (δ, ppm): 7.44–8.22 (s, NH_2, mC_6H_5–CH=N), 11.49 (s, NH); ^{13}C NMR (δ, ppm): 177.81 (C=S), 141.14 (CH=N), 134.26, 133.08, 128.91, 128.65 (aromatic carbon).

Preparation of bis(benzophenone thiosemicarbazone)cadmium(II) iodide (4). The reaction protocol used for **1** was followed. Benzophenone thiosemicarbazone (0.935 g, 3.66 mmol) and CdI_2 (0.671 g, 1.83 mmol) were used, producing a white precipitate **4**, yield 1.572 g (97.88%), mp 91°C.

For $CdI_2C_{28}H_{26}N_6S_2$ calculated, %: Cd, 12.81; C, 38.35; H, 2.98; N, 9.58; S, 7.31.

Found, %: Cd, 12.97; C, 38.54; H, 2.84; N, 9.28; S, 7.14.

IR, cm^{-1}: 3406, 3286 (ν_{NH_2} asymm. and symm.), 3192 (ν_{N-H}), 1592 (ν_{C-N}), 832 (ν_{C-S}).

^1H NMR (δ, ppm): 7.32–8.48 (s, NH_2, mC_6H_5–C=N), 8.63 (s, NH); ^{13}C NMR (δ, ppm): 177.64 (C=S), 149.03 (C=N), 136.26, 131.17, 129.96, 129.77, 128.31, 128.25, 127.56 (aromatic carbons).

CdS nanoparticles. A three-necked flask equipped with a reflux condenser, thermometer and a rubber septum was charged with oleylamine (3.00 g), which was subsequently heated and maintained at an appropriate temperature (190, 230 or 270°C). A suspension of a complex (250 mg) dispersed in tri-*n*-octylphosphine (6 mL) was injected into the heated oleylamine with a glass syringe. The reaction was stopped after an hour, then first washed with methanol then centrifuged; the supernatant was discarded. The washing process was repeated thrice. The samples were dissolved in hexane prior to spectroscopic and TEM analyses. Acetone was used as a dispersing solvent for HRTEM analysis.

RESULTS AND DISCUSSION

The ligands 4-chlorobenzaldehyde thiosemicarbazone and benzophenone thiosemicarbazone were chosen for their ability to complex to Cd(II) without replacing the halide ligands (Scheme S1 and Fig. S1 showing the synthesis and proposed structures of the complexes, are detailed in the ESI). This provides an opportunity to investigate the probable influence of inorganic ligands (bonded directly to the Cd(II) metal centre) towards the shape and morphology of the NPs, as observed in our previous work [33]. In that study the CdS nanostructures obtained from the chloride containing complexes underwent a particle shape transformation from rods to cubes—when the reaction temperature is increased. The iodido-containing complexes gave predominantly nanodendrites, which further formed chain-like structures when an additional halogen (fluoride) is introduced in the organic thiosemicarbazone ligand component. As such, this new work also aims at investigating the effect of replacing the fluoride atom in L2 with chloride atom in L4, as well as the steric factors introduced in L3 as compared to L1 (Fig. 1).

Due to the nature of the comparative study, the preparation of the precursor complexes and the targeted CdS nanoparticles were carried out using identical reaction protocols outlined in our previous report. The complexes were prepared by reacting two equivalents of either L3 or L4 with one equivalent of either

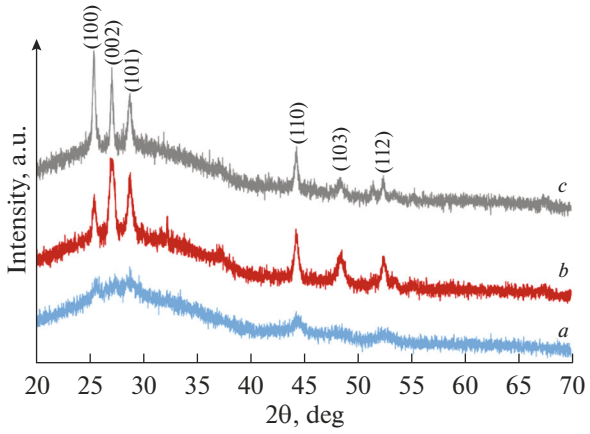

Fig. 2. The p-XRD patterns of oleylamine-capped CdS nanoparticles obtained from chloride-**1** at (a) 190, (b) 230, and (c) 270°C decomposition temperatures.

$CdCl_2$ or CdI_2, thus affording bis(4-chlorobenzaldehyde thiosemicarbazone)cadmium(II) chloride **1**, bis(benzophenone thiosemicarbazone)cadmium(II) chloride **2**, bis(4-chlorobenzaldehyde thiosemicarbazone)cadmium(II) iodide **3** and bis(benzophenone thiosemicarbazone)cadmium(II) iodide **4**. All complexes were confirmed to be analytically pure, using the elemental analysis technique.

These compounds were characterized further by FT-IR and NMR (^1H and $^{13}C\{^1H\}$) spectroscopy, Figs. S2–S13. In the IR spectra, the bands observed in the range of 3400–3200 cm^{-1} are assigned to NH_2 asymmetric and symmetric stretching modes. The N–H stretching mode is observed in range of 3156 to 3192 cm^{-1} IR spectrum. The bands due to ν_{C-N} and ν_{C-S} are observed at 1589 and 957 cm^{-1} for precursor (**1**), 1602 and 837 cm^{-1} for precursor (**2**), 1588 and 955 cm^{-1} for precursor (**3**) and 1592 and 832 cm^{-1} for precursor (**4**) respectively. The values are shifted to lower wavenumbers compared to those in the spectra of free ligands. In the ^1H spectrum of precursors (**1** and **3**) signal due to proton of –NH group is observed at ~11.49 and 8.63 for precursors (**2** and **4**). There is a multiplet at ~7–8 ppm indicates the presence of aromatic protons. These observations are consistent with ligand coordination through azomethine nitrogen and sulphur atoms.

The thermal decomposition of the complexes showed ill temperature transitions of weight loss, mostly two-step degradation mechanism (Fig. S14). The final residues obtained after complete decomposition (maximum temperature set to 600°C) of complexes **1**, **2**, **3** and **4** were approximately 24% (23.7%), 18.5% (20.82%), 13% (18.2%) and 7% (16.5%), respectively. The thermograms show a continuous decomposition as the temperature approaches 600°C, possibly due to residual carbonaceous species in the residues, or a probable sublimation of the cadmium sulfide product.

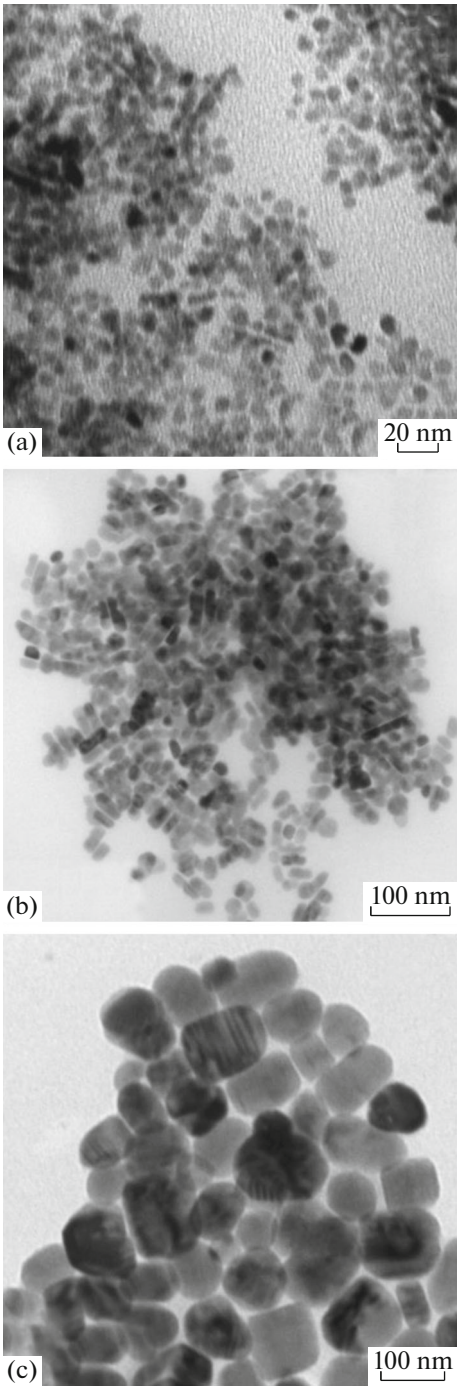

Fig. 3. The TEM micrographs of oleylamine-capped CdS nanoparticles obtained from chloride-**1** at (a) 190, (b) 230, and (c) 270°C decomposition temperatures.

The two-hour thermal decomposition of the complexes under study, in the presence of oleylamine as a high boiling coordinating solvent, afforded yellow-to-orange coloured solid products. As anticipated through our extensive studies on CdS nanomaterials,

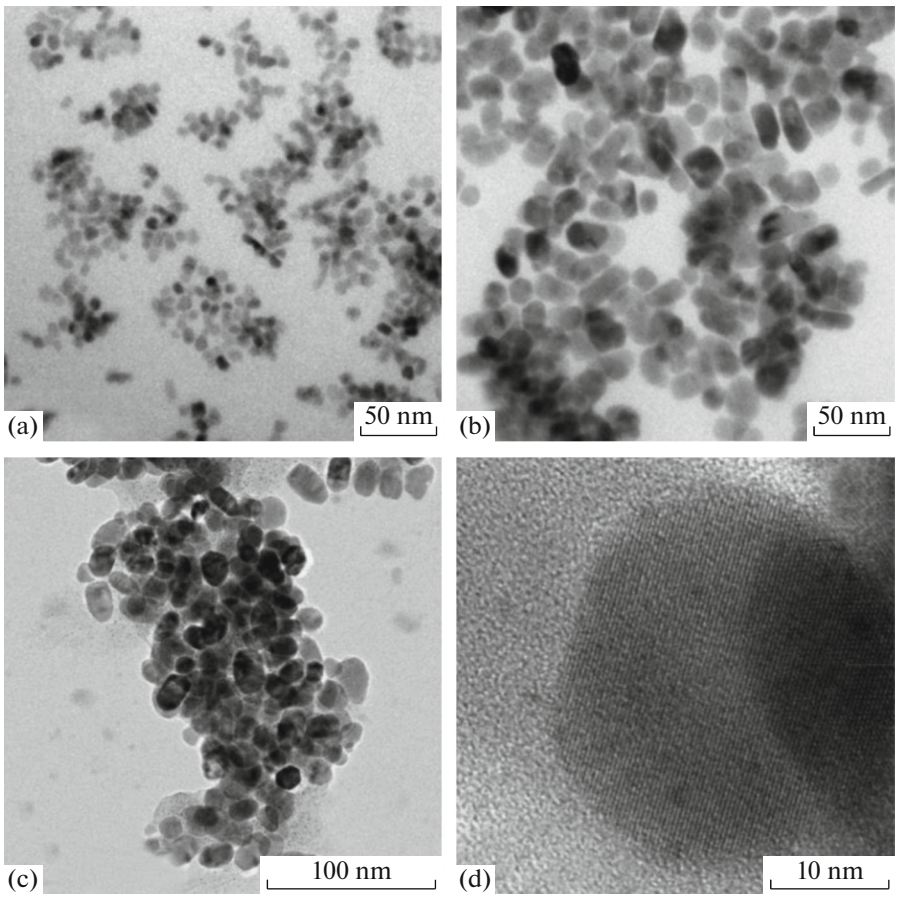

Fig. 4. TEM micrographs of oleylamine-capped CdS nanoparticles obtained from chloride-**2** at (a) 190, (b) 230, (c) 270°C decomposition temperatures, and the HR-TEM micrograph for nanoparticles obtained at 270°C.

we observed a consistent trend on the influence of reaction temperature and nature of the ligands on the crystallographic, morphological and electronic properties of the nanoparticles.

The powder X-ray diffraction (p-XRD) analysis revealed that all products (Figs. 1, S15–S17) from the decomposition reactions match the CdS wurtzite hexagonal phase (JCPDS file no. 03-065-3414), through the identification of the (100), (002), (101), (110), (103) and (112) planes. The peaks in the p-XRD patterns improve in both width and height, as the reaction temperature is increased. This increase in crystallinity as a function of temperature is a well reported trend. It was further observed that the reaction temperature controls the growth of the crystallite towards a certain plane, e.g. the CdS nanoparticles obtained from chloride-**1** at 190°C are amorphous, while an increase in temperature to 230 and 270°C affords nanoparticles whose crystallites prefer to grow along the (002) and (100) planes, respectively, Fig. 2. The benzophenone derivative **2** showed (101) as the preferred growth plane, Fig. S15.

The decomposition of chloride-**1** afforded CdS nanostructures in the form of irregular spheres, rods and cubes at 190, 230 and 270°C reaction temperatures, respectively, Fig. 3. When the bulkier benzophenone thiosemicarbazone ligand is used on chloride-**2**, shape transformation is not significant, Fig. 4. However, at the lower temperature of 190°C there is evidence of early-stage orientated attachment between two irregular sphere-like nanoparticles, forming dumbbell-like nanostructures. An increase in temperature results to elongated and irregular cubic-like nanoparticles, at 230 and 270°C, respectively.

Complex **3**, iodido derivative of **1**, produced nanoparticles exhibiting interesting morphological features. Nanodendrites are obtained at 190°C, which undergo attachment thus forming branching chain-like structures when the temperature is increased to 230°C. A further increase to 270°C, however reduces the formation of the nanodendrites, instead bipod and tripod-like nanoparticles are formed. Furthermore, relatively shorter chain-like structures are obtained. These interesting observations are similar to those of nanoparticles prepared from L2-cadmium(II) iodide reported in our previous work [33]. Interestingly, the chain-like arrangement of the nanodendrites is only observed when the cadmium iodide complexes of hal-

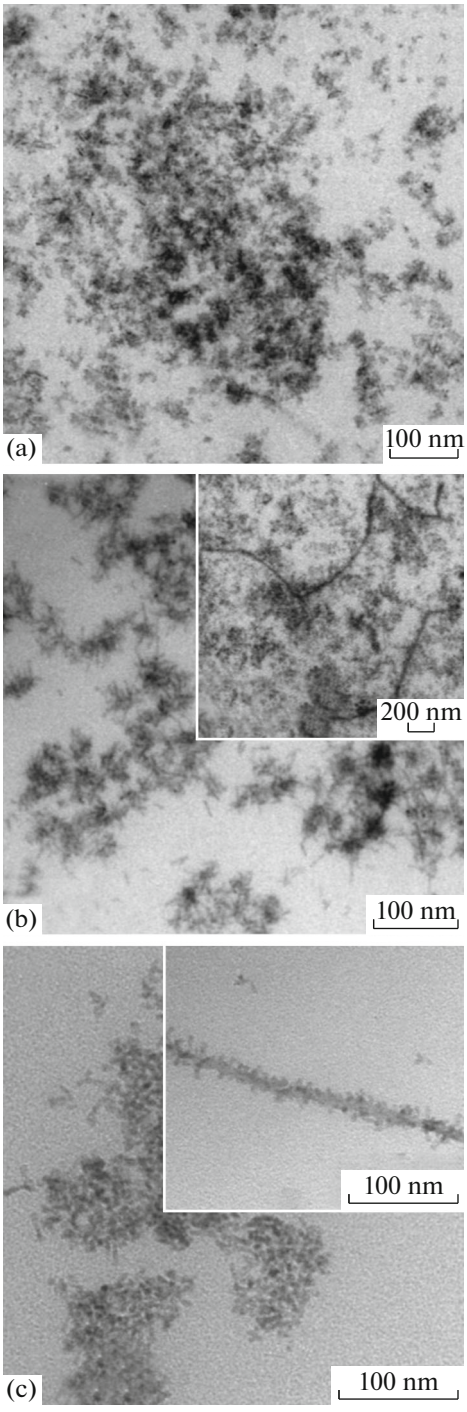

Fig. 5. The TEM micrographs of oleylamine-capped CdS nanoparticles obtained from iodide-**3** at (a) 190, (b) 230, and (c) 270°C decomposition temperatures.

ogen-incorporated thiosemicarbazone ligands (4-fluoroacetophenone L2 and 4-chlorobenzaldehyde L4) are used. The iodide-**4** does not form nanodendrites as observed for the cinnamaldehyde L1 derivative. Instead, flake-like particles are obtained at 190°C, an increase to 230 and 270°C results in cube-like nanoparticles, Fig. 6. We hypothesize that, halogen inclusion (by desorption/adsorption) into CdS nanoparticles influences growth of the particles with such various shapes, of course together with other reaction conditions such as temperature. The work conducted by Manna and co-workers [35] showed that the shape evolution on CdS–CdSe systems were due to an additional role of Cl-containing species in influencing the relative stabilities of various crystal facets of the as-synthesized pods by selective adhesion to certain sets of facets.

The effect of reaction temperature and nature of the complexes on the optical properties of the nanoparticles were investigated. The absorption measurements indicate that the excitonic absorption peaks and band gap energies of the as-prepared nanoparticles vary with reaction temperature, as observed from the representative UV-Vis absorption spectra and Tauc plots in Fig. 7 (i) and (ii), respectively. The shape of the absorption spectra is typical of CdS nanomaterials. This variation in optical properties generally instigate an indirect proportional relationship to the particle size of the materials, i.e. larger band gaps are typical of smaller particle sizes and *vice versa*. Thus, Fig. 8 aims to illustrate this relationship in a graphical approach. At 190°C reaction temperature, all complexes produce nanoparticles with band gap energies between 2.5–2.7 eV, which are blue-shifted relative to 2.42 eV of bulk CdS. The benzophenone thiosemicarbazone complexes, chloride-**2** (Fig. S18) and iodide-**4** (Fig. S20), have larger band gaps compared to the 4-chlorobenzaldehyde thiosemicarbazone counterparts. This may be attributed to the decomposition and/or dissociation of the complexes dominated mostly by steric factors induced by the organic ligands. However, the trend is not observed on the particle sizes, regardless of the difficulties in measuring the particles sizes of nanoparticles fabricated from iodide-**4** at 190°C. Furthermore, the average particle sizes and band gap energies of the nanoparticles obtained from chloride-**1** and iodide-**3** (Fig. S19) do not correlate.

From the previous work, the energy dispersive X-ray spectroscopy analyses did not find traces of the halide ions on the as-prepared nanoparticles, thus, ruling out their direct involvement on the observed morphological and optical properties. The organic component of the complex can easily decompose and be given off as organic compounds, however, the fate of the dissociated halide ligands and interactions with the capping agent are not known in the solvent-based, thermolytic fabrication processes. Literature reports formation of nanoparticles with improved photostability and electronic properties influenced by halogen passivation in the particles [36].

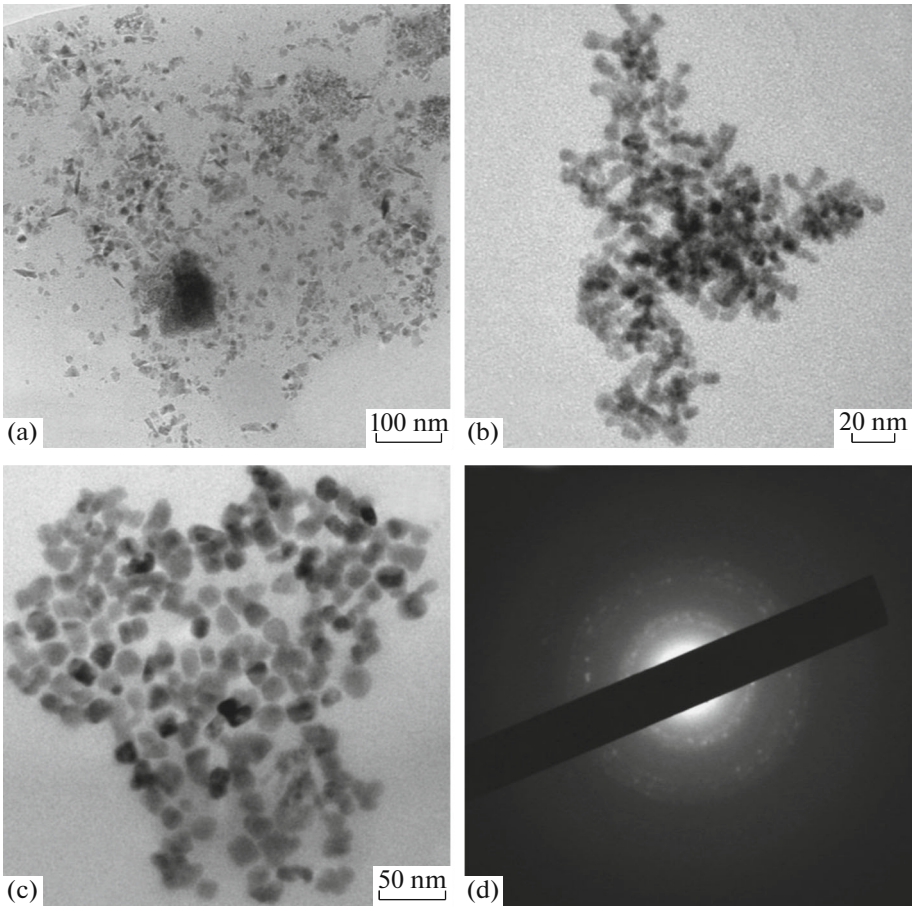

Fig. 6. The TEM micrographs of oleylamine-capped CdS nanoparticles obtained from iodide-**4** at (a) 190, (b) 230, (c) 270°C decomposition temperatures, and the FFT diffraction for nanoparticles obtained at 270°C.

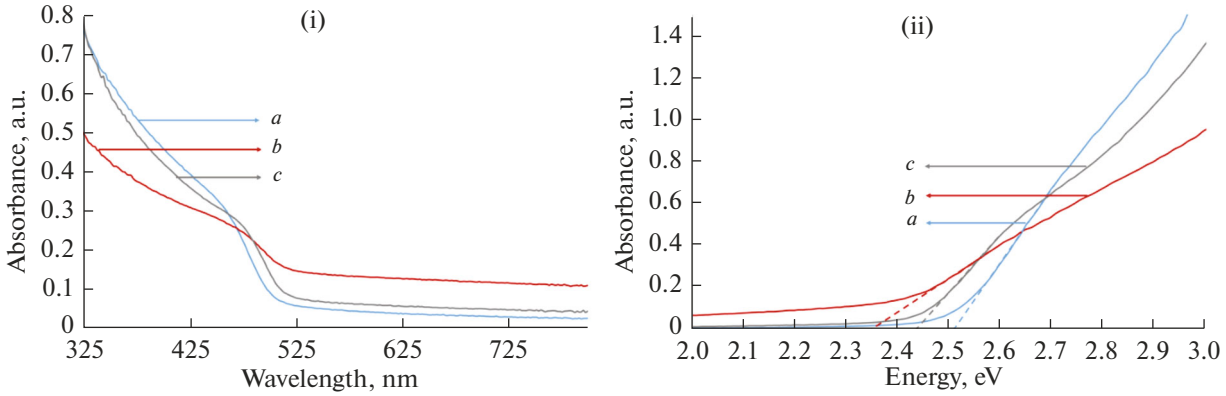

Fig. 7. The (i) UV-Vis absorption spectra, and the corresponding (ii) Tauc plots of the CdS nanoparticles fabricated from chloride-**1** at (a) 190°C, (b) 230°C, and (c) 270°C reaction temperatures.

CONCLUSIONS

The thiosemicarbazone complexes with $CdCl_2$ and CdI_2 have been synthesized, fully characterised and evaluated as potential single source precursors for the fabrication of CdS nanoparticles. The fabrication protocol used was the solvothermal decomposition technique known as thermolysis, using oleylamine as a coordinating solvent. The temperature of the reaction, as well as the nature of the ligands on the complexes were investigated for their influence on the morphological and optical properties of the CdS nanoparticles. The powder XRD recognised reaction tempera-

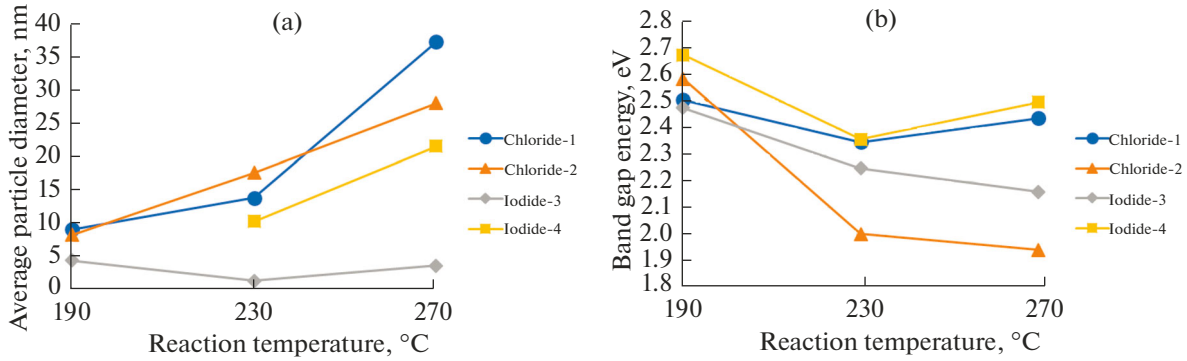

Fig. 8 The comparative graphical representation of (a) average particle sizes (diameter) measured from TEM micrographs (data in Table S1), and (b) the band gap energies estimated from the Tauc plots (data in Table S2).

ture the only parameter to influence the crystallinity of the samples, the crystallographic phase of the nanoparticles was the same for all complexes. The TEM micrographs showed different morphologies ranging from irregular cubes to nanodendritic chains, as a result of temperature and nature of the complexes. The UV-Vis spectra mostly showed blue-shifted absorptions and corresponding band gap energies at lower fabrication temperatures, however no trend was established in relation to the particle sizes obtained from the TEM measurements. Therefore, the overall observations, particularly on the morphological and optical properties, may be due to the passivation efficiency of the capping agent which could be compromised by the presence of the halide ions in the reaction mixture during the fabrication processes. The current work thus provides early-stages data towards understanding the mechanisms involved in such a complex system. Furthermore, the combination of the interesting morphological features and optical properties could be useful for various potential applications such as photocatalytic dyes degradation and photovoltaic devices.

APPENDIX A

Supporting information includes Scheme S1 (synthesis of complexes), proposed chemical structures (Fig. S1), ^{1}H and ^{13}C NMR spectra (Figs. S2–S9), IR spectra (Figs. S10–S13), thermograms (Fig. S14), powder X-ray diffraction patterns (Figs. S15–S17), UV-Vis absorption spectra (Figs. S18–S20), and average particle size diameter (Tables S1, S2) for compounds **1**–**4**.

ACKNOWLEDGMENTS

The authors also thank the Microscopy and Microanalysis Unit (MMU) of the University of KwaZulu-Natal and Council for Scientific and Industrial Research, South Africa for transmission electron microscopy imaging.

FUNDING

The authors are grateful to the National Research Foundation (NRF, Grant number: 64820), South Africa, the India–Brazil–South Africa (IBSA) program, Royal Society-DFID program and the Department of Science and Technology (DST)-PURSE, India, for financial support.

SUPPLEMENTARY MATERIALS

Supplementary materials are available for this article at https://doi.org/10.1134/S0036023619080072 and are accessible for authorized users.

REFERENCES

1. D.-S. Chuu and C.-M. Dai, Phys. Rev. B **45**, 11805 (1992).
2. Y. Guo, J. Wang, Z. Tao, et al., Cryst. Eng. Commun. **14**, 1185 (2012).
3. F. H. Zhao, Q. Su, N. S. Xu, et al., J. Mater. Sci. **41**, 1449 (2006).
4. J. S. Son, K. Park, S. G. Kwon, et al., Small **8**, 2394 (2012).
5. G. Tai, W. Guo, Ultrason. Sonochem. **15**, 350 (2008).
6. S. Dowland, T. Lutz, A. Ward, et al., Adv. Mater. **23**, 2739 (2011).
7. H. Wang, Z. Sun, Q. Lu, F. Zeng, and D. Su, Small **8**, 1167 (2012).
8. M. Kowshik, N. Deshmukh, W. Vogel, et al., Biotechnol. Bioeng. **78**, 583 (2002).
9. M. Antoniadou and P. Lianos, J. Photochem. Photobiol. A: Chem. **204**, 69 (2009).
10. G. B. Shombe, E. B. Mubofu, S. Mlowe, et al., Mater. Sci. Semicond. Process. **43**, 230 (2016).
11. I. Pujalté, I. Passagne, B. Brouillaud, et al., Part Fibre Toxicol. **8**, 10 (2011).
12. M. N. Rhyner, A. M. Smith, X. Gao, et al., Nanomedicine **1**, 209 (2006).
13. C.-Y. Lai, B. G. Trewyn, D. M. Jeftinija, et al., J. Am. Chem. Soc. **125**, 4451 (2003).
14. P. S. Nair, T. Radhakrishnan, N. Revaprasadu, et al., J. Mater. Chem. **12**, 2722 (2002).

15. B. S. Rao, B. R. Kumar, V. R. Reddy, et al., Chalcogenide Lett. **8**, 177 (2011).
16. S. Karan, B. Mallik, J. Phys. Chem. C **111**, 16734 (2007).
17. Z.-X. Cai, H. Yang, Y. Zhang, and X.-P. Yan, Anal. Chim. Acta **559**, 234 (2006).
18. Y. Xia, Y. Xiong, B. Lim, and S. E. Skrabalak, Angew. Chem. Int. Ed. **48**, 60 (2009).
19. M. Green, J. Mater. Chem. **20**, 5797(2010).
20. S. Iravani, Green Chem. **13**, 2638 (2011).
21. L. D. Nyamen, N. Revaprasadu, P. T. Ndifon, Mater. Sci. Semicond. Proc. **27**, 191 (2014).
22. J. W. Kyobe, E. B. Mubofu, Y. M. M. Makame, et al., Physica E **76**, 95 (2016).
23. S. Mlowe, R. Pullabhotla, E. Mubofu, et al., Int. Nano. Lett. **4**, 106 (2014).
24. D. Fan, M. Afzaal, M. A. Malik, et al., Coord. Chem. Rev. **251**, 1878 (2007).
25. L. D. Nyamen, V. S. R. Pullabhotla, A. A. Nejo, et al., New J. Chem. **35**, 1133 (2011).
26. S. Mlowe, D. J. Lewis, M. A. Malik, et al., New J. Chem. **38**, 6073 (2014).
27. V. S. R. Pullabhotla, M. Scriba, N. Revaprasadu, et al., Nanotechnol. **11**, 1201 (2011).
28. N. Pradhan, B. Katz, and S. Efrima, J. Phys. Chem. B **107**, 13843 (2003).
29. A. L. Abdelhady, M. A. Malik, and P. O'Brien, J. Inorg. Organomet. Polym. Mater. **24**, 226 (2014).
30. J. C. Bruce, N. Revaprasadu, and K. R. Koch, New J. Chem. **31**, 1647 (2007).
31. C. Byrom, M. A. Malik, P. O'Brien, et al., Polyhedron **19**, 211 (2000).
32. P. D. McNaughter, S. A. Saah, M. Akhtar, et al., Dalton Trans. **45**, 16345 (2016).
33. A. S. Pawar, S. C. Masikane, S. Mlowe, et al., Eur. J. Inorg. Chem. **366** (2016).
34. F. E. Anderson, C. J. Duca, and J. V. Scudi, J. Am. Chem. Soc. **73**, 4967 (1951).
35. M. R. Kim, K. Miszta, M. Povia, et al., ACS Nano **6**, 11088 (2012).
36. J. Zhang, J. Gao, E. M. Miller, et al., ACS Nano **8**, 614 (2014).